Artificial Neural Network for Microhardness of Al-Mg Based Alloy with Sn Addition

R.H. Nada[a], A.M. Abd El-Khalek[a], F. Abd El-Salam[a], M. Y. El-Bakry[a,b], D.M. Habashy[a] and E. Abd El-Rheim[c]

a. Department of Physics, Faculty of Education, Ain Shams University, Cairo, Egypt
b. Department of Physics, Faculty of Science, University of Tabuk, Saudi Arabia
c. Tabbin Institute for Metallurgical Studies, Helwan, Egypt

asaad_abdelkahlk@yahoo.com, Tel: 0020114249458

Abstract— Artificial neural networks (ANNs) have been applied to age-hardening of microhardness measurements, H_v, were obtained for sheets of Al-3wt.% Mg alloy and its tertiary alloys containing Sn from 0 to 2.5 wt.% in the temperature range 443-503 K, applied loads (10-300 g) and dwell times (10 - 40 s). The age-hardening curves showed off leveling and pronounced oscillations indicating instability which, reflecting a competition between the effect of dynamic recovery or sub-structures coarsening and the effect of solute drag and precipitation hardening. Sn addition, increasing of aging temperature, T, load, L, and dwell time, t, caused a decrease in, H_v, due to the decrease of the amount of free Mg available for further precipitation hardening during the aging process. Rprop algorithm and ANNs were employed to obtain a mathematical formula describing the microhardness measurements. The simulated and predicted results showed good agreement with the experimental data. This study showed that the ANN model and Rprop algorithm are capable of accuracy predicting the age-hardening process in the training and testing phases.

Index Terms— microhardness, dynamic recovery, precipitation hardening, Artificial neural networks (ANNs), Rprop algorithm, Rprop, age-hardening

1 Introduction

There is now a great interest in developing highly formable aluminium alloys and, in particular Al-Mg based alloys. Aluminium alloys with magnesium as the major alloying element which achieve high strength with good ductility through cold work, have been considered for use in a wide variety of applications [1] due to their low density, excellent properties, over all Al alloys, such as high strength, good formability, corrosion resistance and weldability. As wrought non-heat treatable alloys, their strength is derived mainly from solid solution strengthening by Mg which has a substantial solid solubility in Al, and strain hardening [2]. Sn as a minor alloying element in Al alloys [3] can increase the strength by solution strengthening [4]. Sn as unconvential alloying element in reasonable combination with Al and Mg alloys is a basis for advanced applications [5]. In the past, Sn was added to increase the fluidity of casting alloys and presently it is added to alloys for bearings because of its excellent anti-welding characteristics with iron, its low modulus and low strength [6], as providing suitable surface properties [7].

Hardness as a complex property related to the strength of interatomic forces, is defined as the resistance of a material to local plastic deformation. Microhardness testing can be the easiest way to determine the mechanical properties of the different phases of the structure and follow aging behaviour during phase decomposition sequence [8].

Recently, automated techniques [9-14] (based on artificial intelligence approaches) for generating, collecting, and storing data from scientific measurements have become increasing precise and powerful. An artificial neural network (ANN) is a nonlinear computing system consisting of a large number of interconnected processing units (neurons) that simulates human brain learning.

The possibility of using ANN method for modeling the hardness was investigated [15-19]. According to the universal approximation theory [9-14], an ANN with a single, two, three, …, hidden layers with the proper number of hidden neurons can map any nonlinear function to any desired accuracy.

In our work, ANN and back propagation algorithm (Rprop) were employed to simulate and predict the microhardness, H_v, as a function of Sn% addition, aging temperature, T, load, L, and dwell time, t. This paper is organized into five sections. Section 2 provides experimental procedure of solution treatment and aging process. Section 3, gives a review of basics of the ANN technique. Result and discussion are provided in section 4.

2 Experimental Procedure:

Aluminum-Magnesium based alloys containing 3wt.%Mg and tertiary alloys (Al-3wt.%Mg-xwt.%Sn) with x= (0, 0.2, 0.5, 1, 1.5, 2, 2.5) were prepared from elements of 99.9% purity (Al), 99.9 (Mg) and 99.99 Sn. These alloys were prepared by weighting the proper ratios of their components and each composition was melt in graphite crucible placed in the stable zone of a muffle furnace adjusted at 1123K, which is a temperature above the melting point of Al and Mg. When Al is completely melt cleaner material is added to remove all the gases and the impurities inside it, then Mg is added to Al until it completely melt. Finally Sn is added and the casting was carried out in hot iron moulds. The melt was cooled in iced wa-

ter.

All specimens were given an initial annealing for 8h, at 773K and then quenched in cold water. The ingots were rolled with intermediate annealing at 773K to obtain sheets of 7cm length, 3cm width and 0.1cm thickness. The micro-hardness measurements, the Vickers micro-hardness values H_v, were obtained by using (Leco microhardness tester LM 700). The tested sheets were heated for 2h in the working temperature range from 443K to 503K in steps of 10 K, then quenched in cold water kept at room temperature (RT). The surface of any tested sample was polished by using polishing machine (KNUTH-ROTOR 2 STRUERS) then examined by an optical microscope having magnification of 20X and 50X. Hardness indentation was obtained by applying automatically the loads 10, 50, 100 and 300 g for the dwell times 10, 20, 30 and 40 s. The two lines which move at opposite sides of the indentation, were adjusted to the edges of the indentation diagonals and the end button was pressed to show the mean diagonal value and the corresponding hardness value.

3 Artificial Neural Network:

Artificial neural networks [12] ANNs are a portion of "Expert Systems" or "Computational Intelligence Systems" that inspired from the architecture and internal features of the human brain and nervous system. ANNs are consisting of a large number of simple processing elements called as neurons. Their power comes from the parallel processing of the data information that follows from input layer to output layer via neurons" connections as shown in Fig. 1. The Multi-layer feed forward (MLFF) neural network is the most common neural network structure. The relationship between the i th output (y_i) and the inputs ($x_1, x_2, \ldots, x_p$) has the following mathematical representation [13-19]:

$$y_i = h\left[\sum_{j=1}^{q} w_j . g\left(\sum_{i=1}^{p} w_{ij} . x_i + w_{0ij}\right) + w_{0j}\right] \quad (1)$$

where, h and g are activation functions of hidden and output layers respectively; w_{ij} (i = 0,1,2,…,p, j = 1,2,….q) and w_j (j= 0,1,2,….q) are connection weights of network; p and q are the number of nodes at input and hidden layers respectively and w_{0j} and w_{0ij} are biases value of output and hidden layers, respectively.

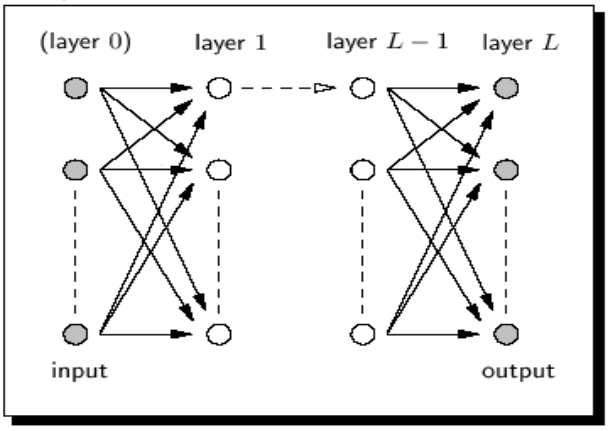

Fig. 1. The general layout of a feed forward neural network

In this technique, the network consists of an input layer, an output layer and a number of hidden layers. At each node in a layer, the information is received, stored, processed, and communicated further to nodes in the next layer. All the weights are initialized to small random numeric values at the beginning of training. These weights are updated or modified iteratively using the generalized delta rule or the steepest gradient descent principle. The training process converges when no considerable change is observed in the values associated with the connection links or when a termination criterion is satisfied [20].

The methodology used for the assessment of network performance involves obtaining the minimum statistical measures of error between experimental data and simulated results (calculated) of hardness by the model. Statistical parameters, namely, Mean Absolute Error (MAE), Root Mean Square Error (RMSE), Standard Error (SE) and coefficient of determination (R^2) represented by equations were used to check the performance of the developed model[21].

A well-trained ANN model should produce small MAE, RMSE and SE with large R^2 values [21]. The ANN model was trained with varying numbers of neurons and randomly chosen logsig (Log sigmoid) transfer functions and Trainrp (Resilient back propagation; Rprop) algorithm for hidden layer.

BP algorithms [12] consist of several training methods such as Quasi-Newton algorithms, Levenberg-Marquardt method, Conjugate Gradient algorithms, Resilient Backpropagation algorithm, etc. All of these algorithms have their benefits and suitable for specified ANNs according to the number of layers, nodes and transfer functions in each layer. We use Resilient Backpropagation algorithm to eliminate harmful effects of squashing functions in the magnitudes of the partial derivatives and for faster training as described elsewhere [11,12,21,22].

4 Results and Discussion:

The leveling off and pronounced oscillations of the age-hardening curves in Fig. 2 (a – d), which were observed previously [6], in these curves beyond 443K, provide a clear indication of instability. The hardness peaks observed for all the curves may correspond to different aging processes. These oscillations are readily understood in terms of competition between a metallurgical reaction concerning the structure variations [23] besides the very effective role of Mg in reducing the rate of creep [24], which tends to increase the hardness and the thermally induced intrinsic decrease in hardness with increasing aging temperature. The hardness therefore never produces the behaviour of homogeneity and stabilization as long as the reaction proceeds to completion until competition comes to an end and then a certain regular behaviour dominates, which is not attained in the curves obtained in the test-

ed temperature range under the applied loads and the dwell times considered. This unstable behaviour cannot be explained here by the onset of recrystallization, which occurs at a temperature higher than 523K [24]. As can be seen from the optical micrographs of the as cast binary and tertiary alloys containing 0.2 and 2 wt.% Sn given in Fig. 3 (a - c), these alloys exhibit a typical dendritic structure. When increasing Sn content, the dendritic structures become more obvious, and the dendrites are gradually refined. Moreover, some rod-like phase accumulates with cluster morphology in the tertiary alloy with 0.2 wt.% Sn and some white particles can also be found. The cumulate rod-like phase decreases but number density of white particles increases. In the alloy containing the highest Sn (2.5 wt.%) the rod-like phase has changed to dissociative morphology, and a semi-continuous phase can be found , which is of lower strength than the rod-like phase. This leads to the softening observed in the alloys containing Sn. It is clear that the refined dendrite is considered a consequence of the increased Sn content, which also change the columnar grains to equiaxed [6].

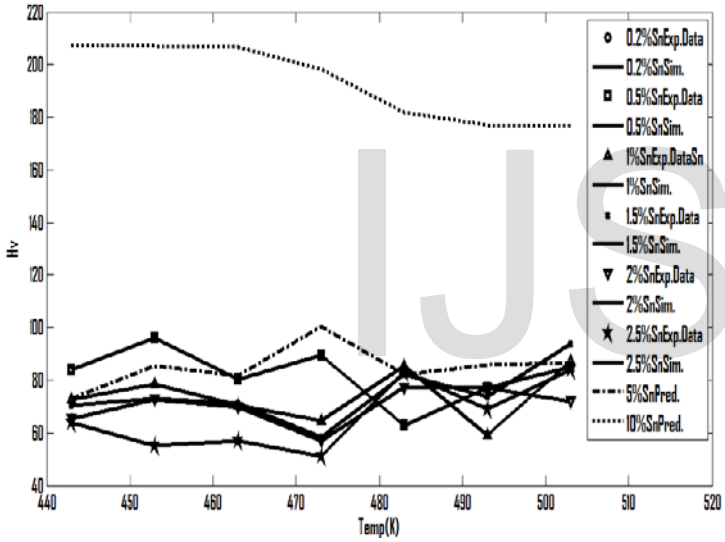

Fig. 2:(a) Temperature dependence of, H_v, under 10g and 10s, and ANN simulation of hardness with temperature.

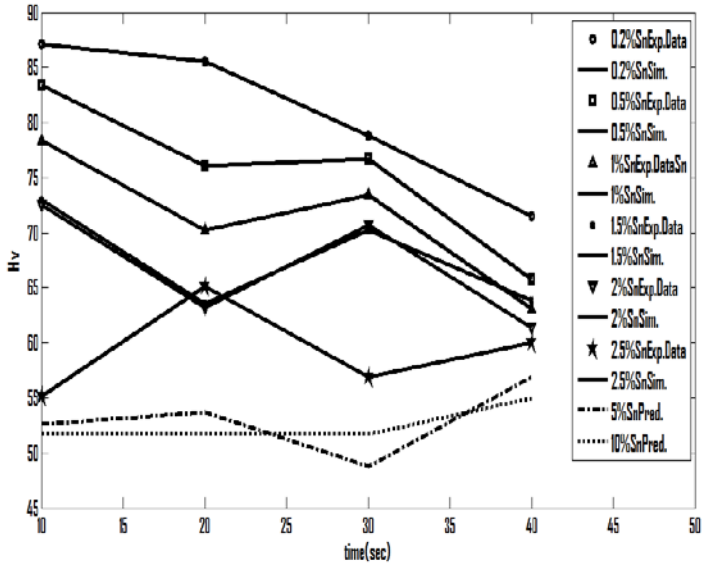

Fig. 2: (b) Dwell time dependence of, H_v, under 10 g at 453K, and ANN simulation of hardness with time.

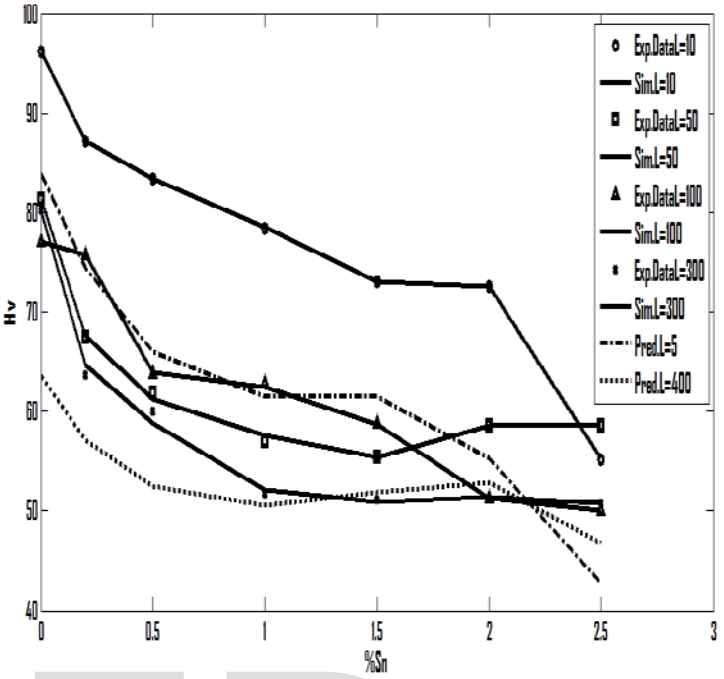

Fig. 2: (c) Sn content dependence of , H_v, under different loads at 453K and 10 s, and ANN simulation of hardness with %Sn at different load.

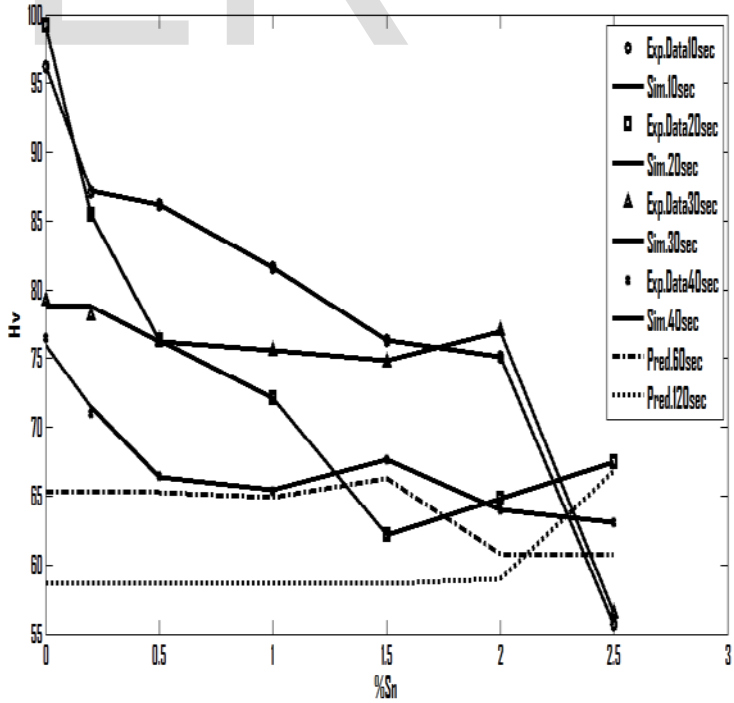

Fig. 2: (d) Sn content dependence of, H_v, under 10 g and different dwell times at 453K, and ANN simulation of hardness with %Sn at different time.

Fig. 4: Block diagram of the four ANN based modeling.

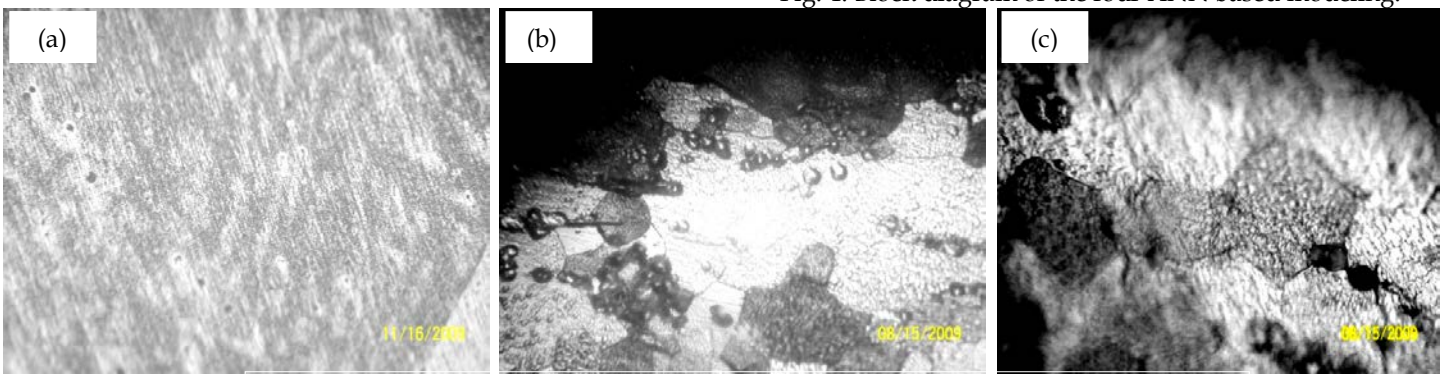

Fig. 3: Optical micrographs with 50X for the samples: (a) Al-3wt.% Mg alloy, (b) Al-3wt.% Mg- 0.2wt.%Sn alloy, and (c) Al-3wt.% Mg 2.5wt.%Sn alloy

.

The experimental data are divided into two sets, namely, training set and validation set. The training set is used to train the ANN model by adjusting the link weights of network model, which should include the data covering the entire experimental space. The inputs of the networks are: (a) temperature, T, and concentration Sn%, (b) dwell time, t, and concentration Sn%, (c) concentration Sn% and loads, L, and (d) concentration Sn% and dwell time, t, while the output is hardness H_v. The validation data set is used to confirm the accuracy of the ANN model. The proposed four individual networks are:

1- The first network was configurated to have inputs (a) and the output is H_v. Fig. 4 represent a block diagram of the four ANN based modeling

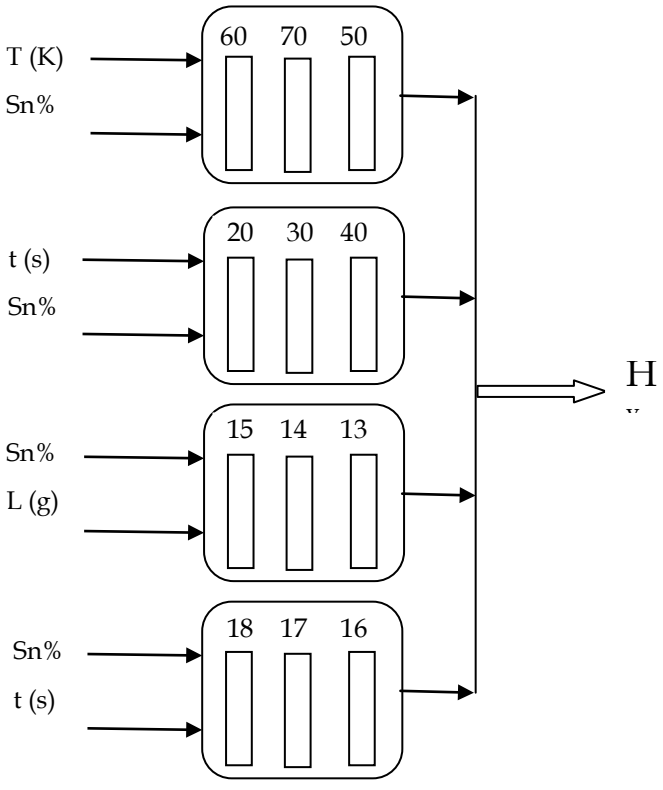

2- Also, second, third and fourth network are configurated to have b,c and d as inputs and the Hv as an output, Fig. 4.

The first ANN having three hidden layers of 60, 70 and 50 neurons, second network: 20, 30 and 40 neurons, third network: 15, 14 and 13 neurons and finally fourth: 18, 17 and 16 neurons respectively. Network performance was evaluated by plotting the ANN model output (H_v) against the experimental data and analyzing the percentage error between the predicted and the experimental data (Fig. 5). In the training process, 91, 129, 800 and 800 epochs was found to be sufficient, Fig. 5, with respect to the minimum error of 8.0829×10^{-6}, 7.8199×10^{-6}, 0.12283 and 0.30925 errors (mean sum of square error MSE). For all networks, the function which describes the nonlinear relationship of the hardness H_v is given in appendix A.

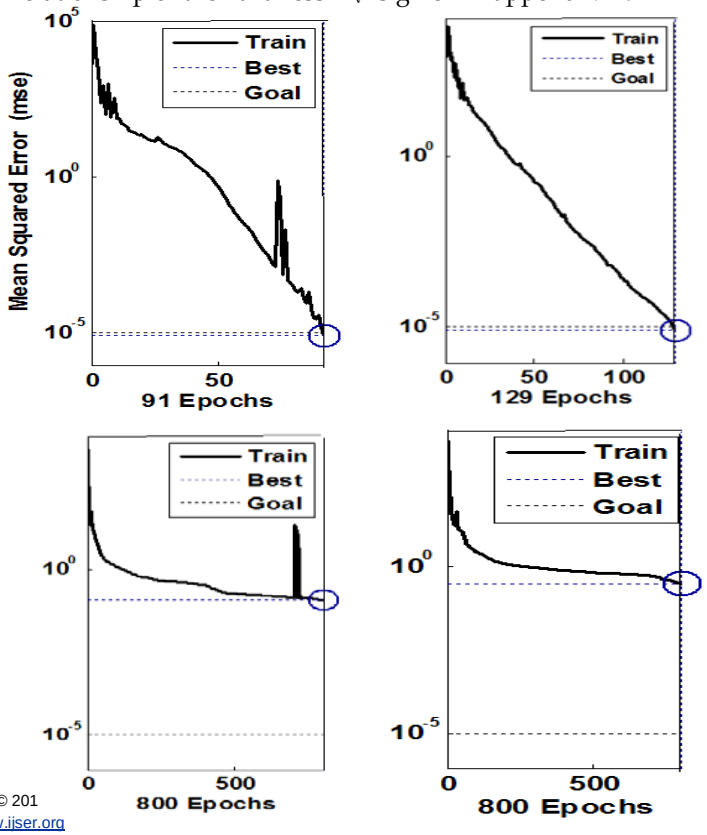

Fig. 5: Performance for hardness using ANN model, where epochs are the number of training

Figure 2 (a-d) shows the simulation results of hardness H_v using our obtained function in appendix A. These figures demonstrate the good agreement between the experimental data and calculated results. Fig. 2a represent the simulation results for H_v with temperature at Sn concentration (0.2 – 10%) using a constant load 10g and time 10 s. ANN simulation of H_v with time as shown in Fig. 2b for different concentration and also for constant load 10 g and temperature 453K. Fig. 2c shows the training of ANN model for H_v versus concentration at different load (10 – 300 g) and constant of time 10s and temperature 453K. The hardness H_v based ANN model against the same concentration for time (10 – 120 s) at constant load 10 g and temperature 453K represented in Fig. 2d. The importance of the obtained function (appendix A) is that they can describe different types of H_v at different temperature, concentration, time and load. Also our obtained function can be used to make predictions about measurements that have not yet been performed.

After the completion of the training stage the testing stage took place. It was found H_v are predicted at concentration (Sn% = 5, 10) in Fig. 2 (a and b), at low and high load (L = 5, 400 g) as in Fig. 2c and at time (t = 60, 120 s) respectively.

The agreement between the predicted and experimental data is especially significant. We also conclude that the ANN models were able to perfectly model and simulate the hardness at different concentration, load and time.

5. Conclusion:

- Age hardening curves of Al-Mg and Al-Mg –Sn alloys showed a leveling off and pronounced oscillations in the temperature range 443-503 K.
- Sn addition induced a decrease in hardness data relative to those of the binary Al-Mg alloy and the tertiary alloys showed a strong.
- In general, increasing temperature, dwell time, applied load and Sn content caused a decrease in hardness.
- The simulated and predicted results of ANN model are perfectly model in mechanical properties of metals and alloys.

Appendix A.

The equation which describes hardness is given by:

H_V = pureline [net. LW{4,3} logsig (net. LW{3,2} poslin (net.LW{2,1} poslin (net. IW{1,1}Tnet. B{1}) net. B{2}) net. B{3}) net. B{4}], where pureline is the linear transfer function, logsig is the log–sigmoid transfer function and poslin is the positive linear function, as shown in the following figure.

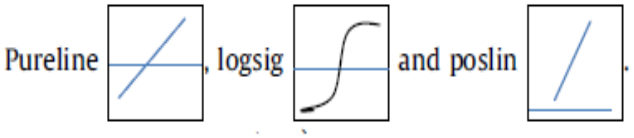

T: the input ,
net. IW{1,1}: linked weights between the input layer and first hidden layer,
net. LW{2,1}: linked weights between the first hidden layer and the second hidden layer,
net. LW{3,2}: linked weights between the second hidden layer and third layer,
net. LW{4,3}: linked weights between the third hidden layer and output layer,
net. B{1}: the bias of the first hidden layer,
net. B{2}: the bias of the second hidden layer,
net. B{3}: the bias of the third hidden layer, and
net. B{4}: the bias of the output layer.

REFERENCES

[1] M.S. Kaiser; Journal of Mechanical Engineering, Vol. 36 (2006) 12-17.

[2] S. P. Wen, Z. B. Xing, H. Huang, Li B. L., W. Wang and Z. R. Nie; Mater. Sci. Eng. A 516 (2009) 42-49.

[3] A. M.A. Mohamed, F.H. Samuel, A.M. Samuel, H.W. Doty and S. Valtierra ; Metal. Mater. Trans. A 39A (2008) 490-495.

[4] X.Wenlong, J. Shusheng, W.Jianli, Y. Jie and W. Limin ; Acta Materiala 56 (2008) 934-941.

[5] J. Gróbner, A. Jonz, A. Koslov, D, Mirkovic, and R. Schmid - Fetzer; Jor. (60) (12) (2008) 32-38.

[6] F. Abd El-Salam, A. M. Abd El-Khalek, R. H. Nada, L. A. Wahab and H. Y. Zahran; Mater. Sci. Eng. A 527 (2010) 1223-1229.

[7] C. J. Kong, P. D. Brown, S. J. Harris, MC Cartney and D. G. ; Mater. Sci. Eng. A 403 (2005) 205-214.

[8] R. S. Sundar, T. R. G. Kutty and D. H. Sastry; Intermetallics 8 (2000) 427-437.

[9] S. Haykin, Neural Networks and learning machine, 3rd ed. Prentic Hall, Upper Saddle River (2008).

[10] Michael Negnevitsky, Artificial Intelligence: A Guide to Intelligent System, Addison Wesley, England, 2005.

[11] H. Igel, M. Husken, Proceedings of the Second International Symposium on Neural Computation, NC'2000, ICSC Academic Press (2000) 115–121.

[12] G. Ghodrati Amiri , P. Namiranian, International journal of optimization in civil engineering , Int. J. Optim. Civil Eng., 3 (1): (2013) 179-207.

[13] H. Erdem, Prediction of the moment capacity of reinforced concrete slabs in fire using artificial neural networks. *Adv Eng Softw*, 41: (2010) 270-276.

[14] M. Khashei, M. Bijari, An artificial neural network (p,d,q) model for time series forecasting. *Expert Syst Appl*, **37**: (2010) 479-89.

[15] M.Y. El-Bakry, A. Moussa, A. Radi, E. El-dahshan, M. Tantawy, Int. J. Sci. Eng. Res. 3 (8) (2012) 15–21.

[16] M.Y. El-Bakry, A. Moussa, A. Radi, E. El-dahshan, D.M. Habashy, G.Abbas Ehab, Int. J. Sci. Eng. Res. 1 (2) (2012)

5–11.
[17] G.M. Behery, A.A. El-Harby, M.Y. El-Bakry, Int. J. Soft Comput. Bioinf. 3 (1) (2012) 1–10.
[18] M.Y. El-Bakry, K.A. El-Metwally, Chaos Solitons Fractals 16/2 (2003) 279–285.
[19] M.Y. El-Bakry, M. El-Helly, Mostafa Y. El-Bakry, Trans. Comput. Sci. III LNCS 5300 (2009) 171–183.
[20] S. Erenturk, and K. Erenturk, Comparison of Genetic Algorithm and Neural Network Approaches for the Drying Process of Carrot. *J. Food. Eng*., 78**:** (2007) 905-912..
[21] P.P. Tripathy and S. Kumar, Neural Network Approach for Food Temperature Prediction During Solar Drying. *Int. J. Thermal Sci.,* 48**:** (2008) 1452-1459.
[23] A. M. Rosenfeld and R. S. Timsit; Phil. Mag. B 49 (2) (1984) 111-126.
[24] L. F Mondolfo; Aluminium Alloys: Structure and properties, Butterworth & Co.(Publishers) ltd, The White Friars Press Ltd, London & Tonbridge. (1976) 311-323.
[22] M. Riedmiller and H. Braun, A direct adoptive method for faster backpropagation learning: Rprop algorithm. In H. Ruspni, editor, proceedings of IEEE- internal conference on neural network (ICNN), Sanfrancisco, (1993) 586- 591